Computer Coupling of Phase Diagrams and Thermochemistry 32 (2008) 423–431

Contents lists available at ScienceDirect

Computer Coupling of Phase Diagrams and Thermochemistry

journal homepage: www.elsevier.com/locate/calphad

Thermodynamic assessment of the Ca–Zn, Sr–Zn, Y–Zn and Ce–Zn systems

Philip J. Spencer [a], Arthur D. Pelton [b], Youn-Bae Kang [b,*], Patrice Chartrand [b], Carlton D. Fuerst [c]

[a] The Spencer Group, 9551, Kingtown Road, Trumansburg, NY 14886, USA

[b] CRCT (Centre de Recherche en Calcul Thermochimique), Département de génie chimique, École Polytechnique, C.P. 6079, succ. Centre-Ville, Montréal, QC, Canada, H3C 3A7

[c] General Motors, MC 480-106-224, 30500 Mound Road, Warren, MI 48090-9055, USA

ARTICLE INFO

Article history:
Received 15 December 2007
Received in revised form
1 March 2008
Accepted 5 March 2008
Available online 1 April 2008

Keywords:
Ca–Zn
Sr–Zn
Y–Zn
Ce–Zn
Quasichemical model

ABSTRACT

Published experimental thermodynamic and phase diagram data for the Ca–Zn, Sr–Zn, Y–Zn and Ce–Zn systems have been critically evaluated to provide assessed thermodynamic parameters for the different phases of the systems. The parameters allow all thermodynamic properties and phase boundaries for each system to be calculated within reasonable error limits. Because a strong compound-forming tendency and pronounced minimum in the enthalpy of mixing curve is observed for the liquid phase of all the systems, the Modified Quasichemical Model (MQM) in the pair approximation has been used throughout the assessment work to treat short-range ordering in the liquid.

1. Introduction

The present assessment work forms part of a Collaborative Research and Development (CRD) Project supported by General Motors of Canada and the National Science and Engineering Research Council of Canada. The aim of the project is to develop new databases and software, which will allow evaluation of the suitability of present and potential new Mg alloys for automotive and aeronautical applications through cost-effective calculations. For Mg alloys, a significant number of relevant thermodynamic assessments have already been carried out through the efforts of several groups worldwide, and two previous publications in the framework of the present project provide thermodynamic descriptions of the six binary and four ternary alloy systems formed from Mg–Ce–Mn–Y [1]. This previously published work forms a basis for the present database development. However, many systems still require assessment and, at the same time, consistency in the thermodynamic modeling used for each system is needed.

Experience shows that alloy systems which show a strong compound-forming tendency in the solid state generally also display a pronounced minimum in the enthalpy of mixing of the liquid phase. Such systems can generally be modeled more reliably using the Modified Quasichemical Model (MQM) for the liquid [2,3]. Of particular importance is the fact that calculations for ternary and higher-order systems, based on quasichemical descriptions of the binaries, have proved to be significantly more reliable than those calculated using other models [1,3]. Many of the magnesium systems being studied in the present project display such characteristics and, for this reason, the MQM is being used for the liquid phase of all systems. A description of the MQM and its associated notation is given in Reference [2]. The same notation is used in the present paper. For all the systems assessed, the coordination numbers Z_{ii} and Z_{jj} for the pure liquid components are taken to be 6. The position of maximum short-range order is given by Z_{ij}/Z_{ji}, as in Table A.2 in the Appendix.

Zinc is an important alloying component of Mg alloys and in the present paper, the assessment work carried out for its binary alloys with the further alloying components Ca, Sr, Y and Ce is described. The results for each system are presented in an abbreviated form in the following sections. Tabulated parameters and crystallographic information for each system are given in Tables A.1 and A.2 in the Appendix.

2. The Ca–Zn system

The Ca–Zn system displays eight intermediate compounds, with pronounced maxima in the liquidus at Zn-rich concentrations (Fig. 1). The available experimental phase diagram data have been reviewed by Itkin and Alcock [4]. Their reported diagram is based mainly on the differential thermal analysis (DTA) measurements of Messing et al. [5], but with modification of the compounds Ca_7Zn_4, Ca_7Zn_{20} to Ca_5Zn_3, and $CaZn_3$ based on later crystallographic information.

* Corresponding author. Tel.: +1 514 340 4711; fax: +1 514 340 5840.
E-mail address: youn-bae.kang@polymtl.ca (Y.-B. Kang).

0364-5916/$ – see front matter © 2008 Elsevier Ltd. All rights reserved.
doi:10.1016/j.calphad.2008.03.001

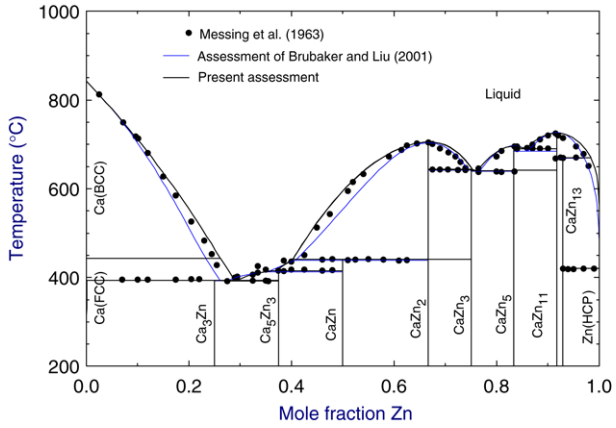

Fig. 1. Ca–Zn phase diagram.

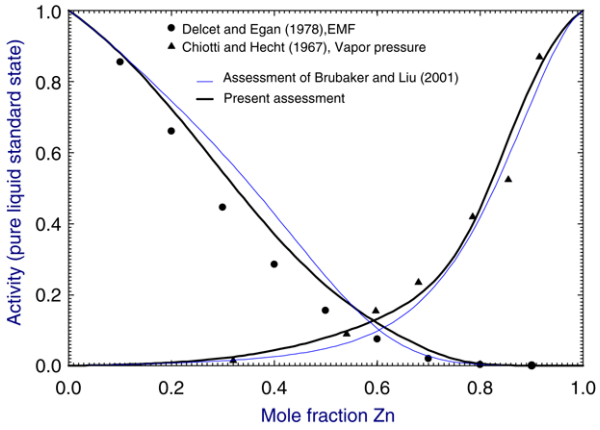

Fig. 2. Calculated and experimental activities for liquid Ca–Zn alloys at 800 °C.

A thermodynamic assessment of the system, using a Bragg–Williams (random mixing) model for the liquid phase, has been carried out previously by Brubaker and Liu [6].

Delcet and Egan used an emf technique with CaF_2 as solid electrolyte to determine Ca activities in the liquid phase at 800 °C [7], while activities of Zn in liquid alloys were obtained by Chiotti and Hecht from dew point studies for alloys with Zn concentrations greater than 50 at.% and from Knudsen effusion measurements for alloys at lower Zn concentrations [8]. No direct calorimetric values are available for the enthalpies of formation of solid or liquid alloys, but enthalpies of formation for the compounds in the system were obtained from the temperature dependence of the experimental Zn vapor pressure data [8]. Chiotti et al. have also used an adiabatic calorimeter to measure the enthalpy of fusion of $CaZn_2$ [9].

All of the above experimental data have been used in obtaining optimized thermodynamic parameters for the phases of the Ca–Zn system. The liquid phase was modeled using the MQM with a maximum short-range ordering composition at a ratio of Zn/Ca = 2:1. It was found that selection of this ordering composition for all of the Me–Zn systems assessed in this work (except Y–Zn) allowed an optimum fit of experimental liquidus data and enthalpies of mixing for the liquid phase where available, with use of a minimum number of parameters. The ordering composition also closely reflects the composition of maximum stability in the solid state, as indicated by the minimum value of the Gibbs energy of formation. The solid compound phases including Ca and Zn were treated as being stoichiometric.

The phase diagram calculated using the optimized parameters is shown in Fig. 1. Experimental data from Messing [5] and the phase boundaries calculated from the assessment due to Brubaker and Liu [6] are also included for comparison.

The calculated activities in the liquid phase at 800 °C are shown together with the experimental data from Delcet and Egan [7] and from Chiotti and Hecht [8] in Fig. 2. Curves from the assessment of Brubaker and Liu [6] are also included for comparison.

The agreement between experimental and calculated values for Zn is good, but the experimental data for Ca lie below the values obtained from the assessment. Since the Gibbs–Duhem equation must be obeyed for the two components, it is not possible to fit simultaneously both experimental activity curves within their experimental uncertainty limits.

The enthalpies of formation at 298.15 K calculated using the present assessed parameters are compared in Fig. 3 with the values derived by Chiotti and Hecht [8] from their Zn vapor pressure data. The present assessed values are identical to those proposed by Brubaker and Liu [6].

The calculated enthalpy and entropy of mixing curves for the liquid phase of the Ca–Zn system are shown in Figs. 4 and 5.

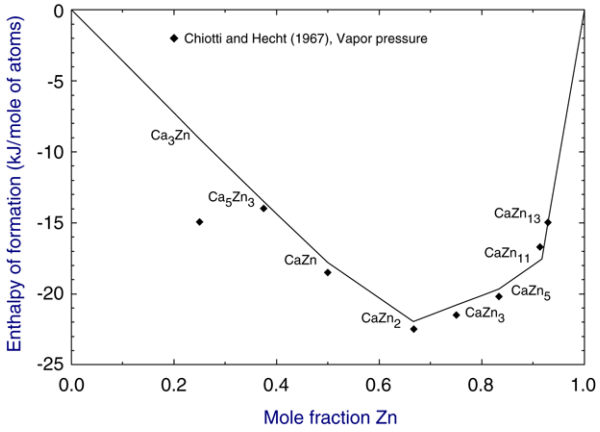

Fig. 3. Enthalpies of formation at 25 °C for the compounds in the Ca–Zn system.

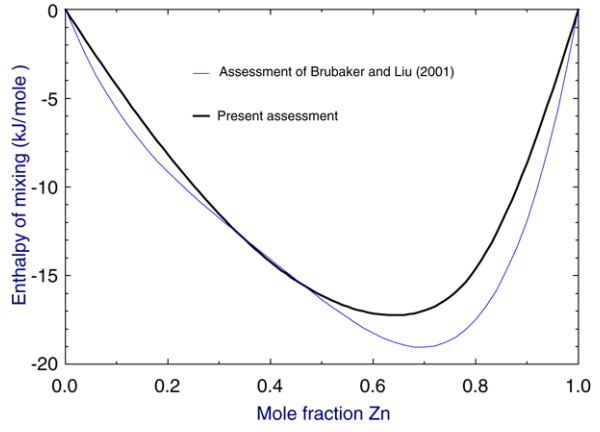

Fig. 4. Enthalpy of mixing of liquid Ca–Zn alloys at 900 °C.

Comparison is made in each case with the assessment due to Brubaker and Liu [6].

A general observation is that the MQM gives a sharper minimum and more nearly linear terminal regions in the enthalpy of mixing curve than are obtained using other models. Although the absolute values of ΔH_{mix} may be very similar, it is frequently found that the partial enthalpies of mixing in limiting composition regions are very different. For example, ΔH_{Zn} at $X_{Ca} = 1$ in Fig. 4 is −44.7 kJ/mol using the MQM (present assessment) and approximately −66 kJ/mol using the Bragg–Williams Model (Brubaker & Liu) [6]. These differences can have a profound effect on calculated solubilities, vapor pressures, and other properties of

Table 1
Invariant reactions in the Ca–Zn system

Invariant reaction	Experimental values [5]				Calculated values[a]			
	T (°C)	X_1	X_2	X_3	T (°C)	X_1	X_2	X_3
Liq + Ca = Ca_3Zn	394	0.273	0.000	0.250	393.4	0.289	0.000	0.250
					392.8	*0.261*	*0.000*	*0.250*
Liq = Ca_3Zn + Ca_5Zn_3	391	0.274	0.250	0.375	392.4	0.291	0.250	0.375
					391.9	*0.273*	*0.250*	*0.375*
Liq + CaZn = Ca_5Zn_3	414	~0.350	0.500	0.375	414.8	0.369	0.500	0.375
					412.7	*0.352*	*0.500*	*0.375*
Liq + $CaZn_2$ = CaZn	439	~0.425	0.667	0.500	439.5	0.402	0.667	0.500
					437.7	*0.406*	*0.667*	*0.500*
Liq = $CaZn_2$	704	0.667	0.667		705.1	0.667	0.667	
					703.4	*0.667*	*0.667*	
Liq = $CaZn_2$ + $CaZn_3$					643.4	0.753	0.667	0.750
					641.1	*0.746*	*0.667*	*0.750*
Liq = $CaZn_3$ + $CaZn_5$	638	0.764	0.750	0.833	640.6	0.762	0.750	0.833
					638.4	*0.764*	*0.750*	*0.833*
Liq = $CaZn_5$	695	0.833	0.833		695.2	0.833	0.833	
					696.5	*0.833*	*0.833*	
Liq = $CaZn_5$ + $CaZn_{11}$	690	0.864	0.833	0.917	689.2	0.856	0.833	0.917
					684.4	*0.863*	*0.833*	*0.917*
Liq = $CaZn_{11}$	724	0.917	0.917		724.9	0.917	0.917	
					726.4	*0.917*	*0.91*	
Liq + $CaZn_{11}$ = $CaZn_{13}$	669	~0.970	0.917	0.929	670.3	0.983	0.917	0.929
					668.2	*0.969*	*0.917*	*0.929*
Liq = Zn + $CaZn_{13}$	420	~1.000	1.000	0.929	419.6	1.000	1.000	0.929
					419.8	*1.000*	*1.000*	*0.929*

X = mol fraction Zn.
[a] Values in regular type are from the present assessment. Values in italics are assessed values reported by Brubaker and Liu [6].

Table 2
Enthalpy of fusion of the $CaZn_2$, $CaZn_5$ and $CaZn_{11}$ phases (J/mol)

Phase	ΔH_{fus} (expt) [9]	ΔH_{fus} (calc) [6]	ΔH_{fus} (calc) present
$CaZn_2$	38 700	34 170	38 316
$CaZn_5$		82 815	86 146
$CaZn_{11}$		227 835	214 451

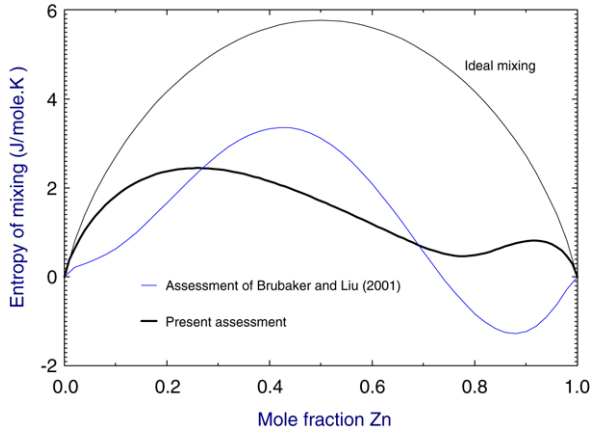

Fig. 5. Entropy of mixing of liquid Ca–Zn alloys at 900 °C.

practical importance when the two models are used as the basis for extrapolations into ternary and higher-order systems.

Table 1 presents a comparison of experimental and calculated compositions and temperatures for the invariant reactions in the Ca–Zn system.

Table 2 presents calculated enthalpies of fusion for the $CaZn_2$, $CaZn_5$ and $CaZn_{11}$ phases. Comparison is made with the corresponding assessed values reported by Brubaker and Liu [6] and the experimental value for $CaZn_2$ reported by Chiotti et al. [9].

3. The Sr–Zn system

The Sr–Zn system displays the four stoichiometric compounds SrZn, $SrZn_2$, $SrZn_5$, and $SrZn_{13}$. The accepted phase diagram is due mainly to Bruzzone and Merlo who used DTA, metallographic and X-ray methods to determine the phase boundaries [10]. Additional measurements of the solubility of Sr in liquid Zn have been made by Shunk, using a metallographic method [11], and by Volkovich et al. using an emf technique in the range from 0.1 to 4 at.% Sr [12].

No experimental calorimetric studies of the system have been made. It is therefore necessary to use comparison of available phase diagram information in conjunction with the thermodynamic properties of the Ca–Zn system to estimate enthalpies of formation in the Sr–Zn system.

A previous thermodynamic assessment of the Sr–Zn system, using a Bragg–Williams (random mixing) model for the liquid phase, has been carried out by Zhong et al. [13].

The liquid phase was modeled here using the MQM with a maximum short-range ordering composition at a ratio of Zn/Sr = 2:1. The solid compound phases including Sr and Zn were treated as being stoichiometric.

The phase diagram calculated using the optimized parameters is shown in Fig. 6. Experimental data from Bruzzone and Merlo [10], from Volkovich et al. [12] and the phase boundaries calculated from the assessment due to Zhong et al. [13] are also included for comparison.

The enthalpies of formation at 298 K calculated using the present assessed parameters are compared in Fig. 7 with the values resulting from the assessment due to Zhong et al. [13].

The calculated enthalpy and entropy of mixing curves for the liquid phase of the Sr–Zn system at 900 °C are shown in Figs. 8 and 9. Comparison is made in each case with the corresponding values from Zhong et al. [13].

Table 3 presents a comparison of experimental and calculated compositions and temperatures for the invariant reactions in the Sr–Zn system.

4. The Y–Zn system

The Y–Zn phase diagram was established largely by the thermal analysis, metallographic and X-ray studies due to Chiotti et al. [14]. Later crystallographic investigations by Harsha [15], Veleckis et al. [16], Bruzzone et al. [17], Fornasini [18] and

Table 3
Invariant reactions in the Sr–Zn system

Invariant reaction	Experimental values [10]				Calculated values[a]			
	T (°C)	X_1	X_2	X_3	T (°C)	X_1	X_2	X_3
Liq + Sr(fcc) = SrZn	369	0.325	0.000	0.500	372.5	0.302	0.0029	0.500
					369.5	*0.307*	*0.002*	*0.500*
Liq + $SrZn_2$ = SrZn	434	~0.470	0.667	0.500	427.6	0.424	0.667	0.500
					432.6	*0.467*	*0.667*	*0.500*
Liq = $SrZn_2$	575	0.667	0.667		577.5	0.667	0.667	
					574.3	*0.667*	*0.667*	
Liq = $SrZn_2$ + $SrZn_5$(lt)	554	0.725	0.667	0.833	557.5	0.719	0.667	0.833
					554.5	*0.719*	*0.667*	*0.833*
$SrZn_5$(lt) = $SrZn_5$(ht)	620	0.833	0.833		619.3	0.833	0.833	
					619.7	*0.833*	*0.833*	
Liq + $SrZn_{13}$ = $SrZn_5$(ht)	650	~0.810	0.929	0.833	656.8	0.801	0.929	0.833
					650.0	*0.794*	*0.929*	*0.833*
Liq = $SrZn_{13}$	830	0.929	0.929		826.5	0.929	0.929	
					830.0	*0.929*	*0.929*	
Liq = $SrZn_{13}$ + Zn(hcp)	420	1.000	0.929	1.000	419.6	1.000	0.929	1.000
					419.7	*1.000*	*0.929*	*1.000*

X = mol fraction Zn.
[a] Values in regular type are from the present assessment. Values in italics are from the assessment due to Zhong et al. [13].

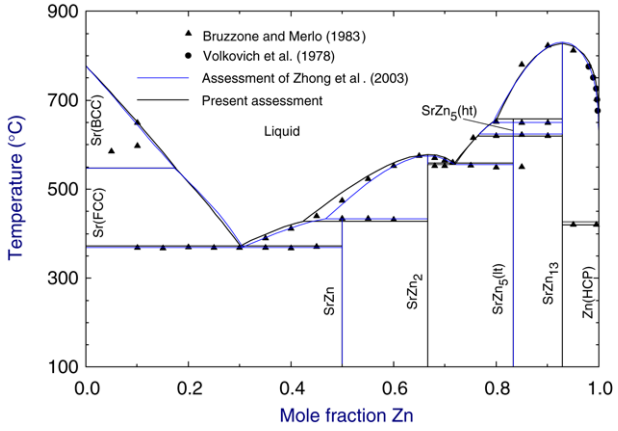

Fig. 6. The Sr–Zn phase diagram.

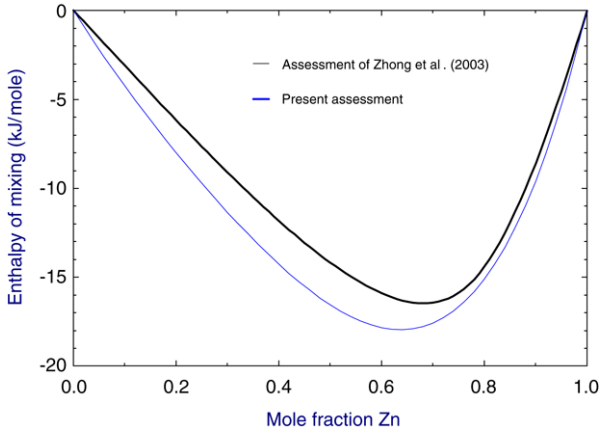

Fig. 8. Enthalpy of mixing of liquid Sr–Zn alloys at 900 °C.

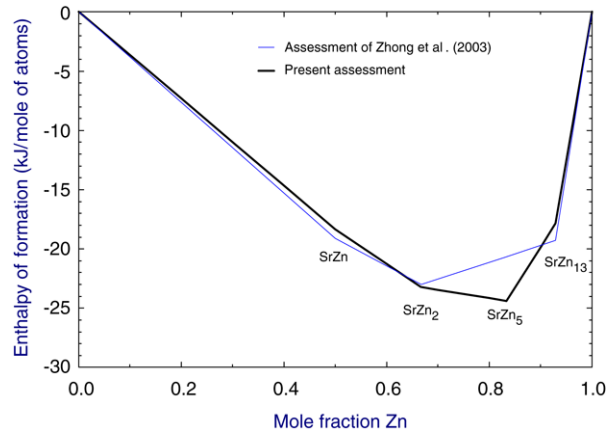

Fig. 7. Enthalpies of formation at 25 °C for the compounds in the Sr–Zn system.

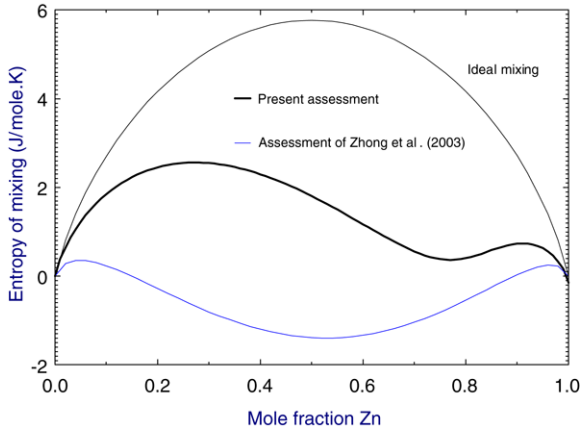

Fig. 9. Entropy of mixing of liquid Sr–Zn alloys at 900 °C.

Ryba [19] suggested that some amendments to the stoichiometries of the phases reported by [14] were necessary, and further phase boundary investigations by Mason and Chiotti resulted in additional small changes to the phase boundaries of the system [20]. Butorov et al. [21] obtained values for the solubility of Y in liquid Zn from emf studies of Zn-rich alloys. The system is characterized by eight compounds and three maxima in the liquidus.

Thermodynamic values for the compounds in the system have been determined by Mason and Chiotti using the dew point vapor pressure method [20] in the temperature range 452–1017 °C (depending on alloy composition). Their results supersede the data reported by [14]. Hoshino and Plambeck carried out emf studies of Zn-rich alloys in the temperature range 450–570 °C to obtain thermodynamic data for YZn_{12} [22]. Similar measurements were made by Butorov et al. in the temperature range 675–800 °C for alloys containing 0.2 to 0.8 at.% Y [21] and by Yamschikov et al. for

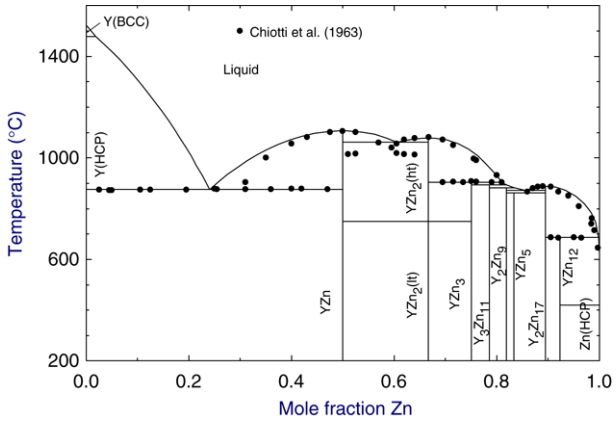

Fig. 10. The Y–Zn phase diagram.

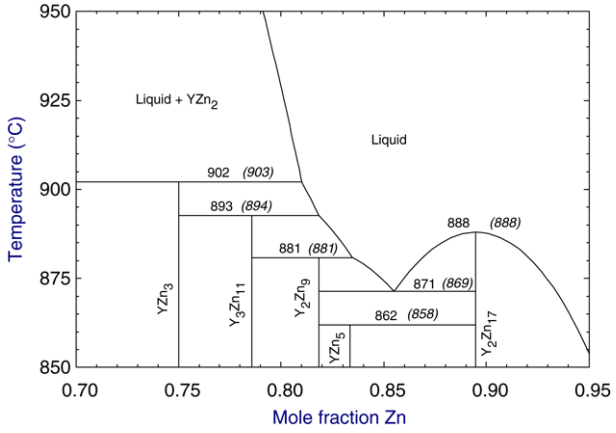

Fig. 11. Enlarged region of the Y–Zn phase diagram (Invariant temperatures in parentheses are from the ASM compilation [27]).

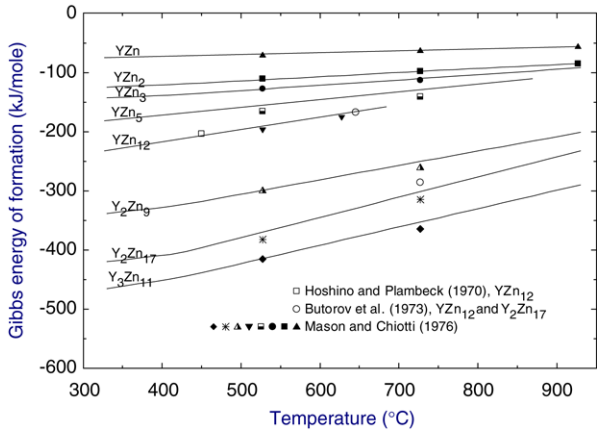

Fig. 12. Gibbs energies of formation of the compounds in the Y–Zn system.

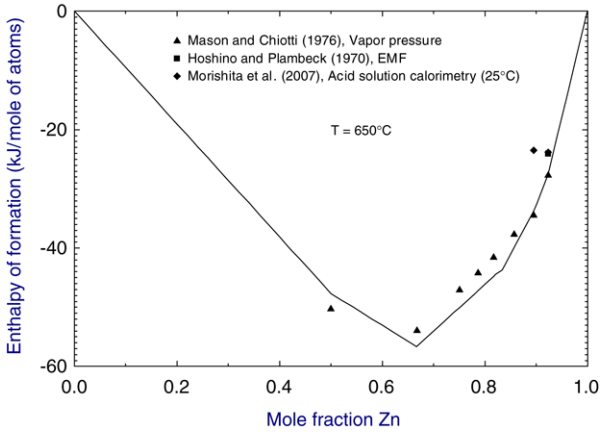

Fig. 13. Enthalpies of formation at 650 °C for the compounds in the Y–Zn system. Reference states are Y(hcp) and Zn(liquid).

saturated solutions in the temperature range 450–800 °C [23]. The specific heat measurements carried out by Marquina et al. [24] for the compound Y_2Zn_{17} only apply to the temperature range 0.3 to 150 K and are therefore not incorporated in the present work.

Morishita et al. have recently determined enthalpies of formation and entropies at 298 K for Y_2Zn_{17} and YZn_{12} using acid solution and relaxation calorimetry, respectively [25]. They used their results to calculate the standard Gibbs energies of formation of the two compounds.

A thermodynamic assessment of the system has been reported recently by Shao et al. [26].

Results from all of the above experimental studies were taken into account in the present assessment work. The liquid phase was modeled using the MQM with a maximum short-range ordering composition at a ratio of Zn/Y = 3:2. It was found that selection of this ordering composition allowed an optimum fit of experimental liquidus data using a minimum number of parameters. The solid compound phases including Y and Zn were treated as being stoichiometric.

The phase diagram calculated using the optimized parameters is shown in Fig. 10. Experimental data from Mason and Chiotti [20] are also included for comparison.

Fig. 11 presents an enlarged region of the calculated phase diagram between 70 and 95 mol fraction Zn. Invariant temperatures selected by ASM in their compilation of binary alloy phase diagrams [27] are included for comparison.

The Gibbs energies of formation of the compounds in the system as a function of temperature, calculated using the present assessed parameters, are compared in Fig. 12 with the experimental values resulting from the measurements of Mason and Chiotti [20], Butorov et al. [21] and Hoshino and Plambeck [22]. The Gibbs energy of transformation between YZn_2(lt) and YZn_2(ht) was estimated from the vapor pressure measurement of Mason and Chiotti [20].

Fig. 13 compares the enthalpies of formation at 650 °C, calculated using the present assessed parameters, with values derived from the experiments of Mason and Chiotti [20], Hoshino and Plambeck [22], Morishita et al. [25], and with values from the assessment due to Shao et al. [26].

The experimental values obtained by Morishita et al. [25] appear to be somewhat less accurate in that the reported enthalpy and Gibbs energy of formation of the compound $Zn_{12}Y$ are more exothermic than the corresponding values for $Zn_{17}Y_2$. This seems improbable from the form of the phase diagram and from the conclusions of other experimental and assessment work. Fig. 13 also shows that enthalpies of formation obtained from the assessment due to Shao et al. [26] are somewhat less exothermic than the reported data.

The calculated enthalpy and entropy of mixing curves for the liquid phase of the Y–Zn system at 1600 °C are shown in Figs. 14 and 15.

Table 4 compares experimental partial excess Gibbs energies of yttrium obtained by Butorov et al. [21] and by Yamschikov et al. [23] for Zn-rich alloys with the corresponding values calculated using the present assessed parameters.

The tabulated data show that there is reasonable agreement between experimental results and values calculated using the assessed parameters, particularly for temperatures in the middle

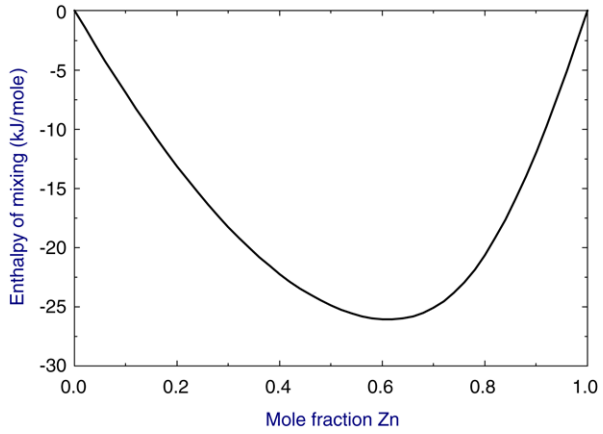

Fig. 14. Enthalpy of mixing of liquid Y–Zn alloys at 1600 °C.

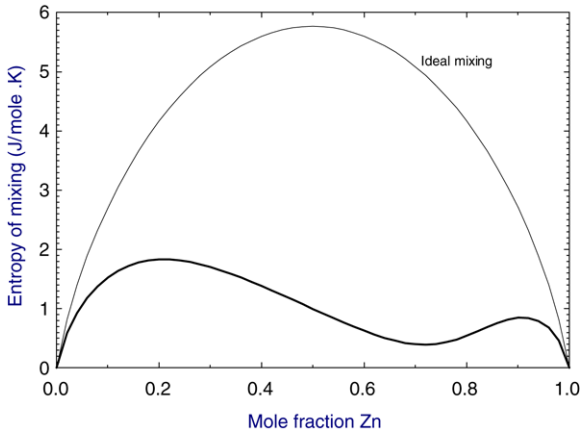

Fig. 15. Entropy of mixing of liquid Y–Zn alloys at 1600 °C.

Table 4
Partial excess Gibbs energy of Y in liquid Y–Zn alloys (kJ/mol)

X_Y	T (°C)	G_Y^E (expt. [23])	G_Y^E (expt. [21])	G_Y^E (calc.)
0.002	675		−121	−109
	690		−118	−109
	720		−112	−108
	760		−105	−108
	800		−98	−107
0.004	675		−120	−108
	690		−118	−108
	720		−112	−108
	760		−105	−107
	800		−98	−107
0.008	675		−120	−107
	690		−118	−107
	720		−112	−107
	760		−105	−106
	800		−98	−106
<0.004	700	−126		−108

of the experimental temperature range. However, it should be pointed out that the experimental data from [21,23] correspond to unreasonably large limiting partial excess entropies of yttrium of approximately −184 J/mol K and −72 J/mol K, respectively, while the present assessment gives a much more reasonable value of about −16 J/mol K.

Table 5 presents the calculated compositions and temperatures for the invariant reactions in the Y–Zn system using the present assessed parameters.

Table 5
Invariant reactions in the Y–Zn system

Invariant reaction	Calculated values			
	T (°C)	X_1	X_2	X_3
Liq = Y(hcp) + YZn	875	0.240	0.000	0.500
Liq = YZn	1106	0.500	0.500	
Liq = YZn + YZn_2	1060	0.605	0.500	0.667
Liq = YZn_2	1078	0.667	0.667	
Liq + YZn_2 = YZn_3	902	0.810	0.667	0.750
Liq + YZn_3 = Y_3Zn_{11}	893	0.818	0.750	0.786
Liq + Y_3Zn_{11} = Y_2Zn_9	881	0.834	0.786	0.818
Liq = Y_2Zn_9 + Y_2Zn_{17}	871	0.855	0.818	0.895
Y_2Zn_9 + Y_2Zn_{17} = YZn_5	862	0.818	0.895	0.833
Liq = Y_2Zn_{17}	888	0.895	0.895	
Liq + Y_2Zn_{17} = YZn_{12}	685	0.998	0.895	0.923
Liq = YZn_{12} + Zn	420	1.000	0.923	1.000

X = mol fraction Zn.

5. The Ce–Zn system

The Ce–Zn phase diagram has been determined largely by Chiotti and Mason [28] using metallographic, thermal, X-ray, and vapor pressure techniques. Their diagram is reproduced in the ASM compilation of binary alloy phase diagrams [27], but with slight changes in stoichiometry of three of the compound phases ($Ce_{13}Zn_{58}$ for Ce_2Zn_9 [29], $CeZn_5$ for Ce_4Zn_{21} [30], and Ce_3Zn_{22} for $CeZn_7$ [31]). There are very close similarities between the stoichiometries of the compounds formed in the Y–Zn and Ce–Zn systems.

The dew-point vapor pressure studies carried out by Chiotti and Mason [28] in the temperature range 550–1040 °C provide the only thermodynamic values available for the compounds in the Ce–Zn system. Their temperature dependent equations for the Gibbs energy of formation of the compounds allow corresponding enthalpies and entropies of formation to be derived.

The emf measurements for Zn-rich liquid alloys performed by Johnson and Yonco [32] in the temperature range 437–745 °C provide the Gibbs energy of formation of $CeZn_{11}$ as a function of temperature and have been used by the authors to derive an enthalpy and entropy of formation for this compound.

Emf studies of Zn-rich liquid alloys containing up to 5.6 at.% Ce have also been carried out by Lebedev and co-workers [33,34] in the temperature range 450–717 °C. Their results provide values of the activity coefficient of Ce in liquid Zn as well as derived values for the partial enthalpy and entropy of solution of Ce in Zn-rich solutions.

No calorimetric studies providing enthalpies of formation of solid or liquid alloys have been found in the literature.

Results from all of the above experimental studies were taken into account in the present assessment work. The liquid phase was modeled using the MQM with a maximum short-range ordering composition at a ratio of Zn/Ce = 2:1. The solid compound phases including Ce and Zn were treated as being stoichiometric.

The Ce–Zn phase diagram calculated using the optimized parameters for the system is shown in Fig. 16, where comparison is made with the experimental points from Chiotti et al. [28].

Fig. 17 compares the assessed enthalpies of formation at 500 °C of the compounds in the Ce–Zn system with values derived from the vapor pressure studies of Chiotti et al. [28] and from the emf studies of Johnson and Yonco [32] and Lebedev et al. [33].

The calculated Gibbs energies of formation of the Ce–Zn compounds at 500 °C are shown in Fig. 18, together with experimental values from Chiotti et al. [28] and Johnson and Yonco [32]. It was found difficult to achieve a more satisfactory agreement between the assessed and experimental values without the resulting enthalpies and entropies of formation having unlikely values. Further experimental information and additional assessment work may be needed to resolve this problem.

Table 6
Partial excess Gibbs energy of Ce in liquid Ce–Zn alloys (kJ/mol)

X_{Ce}	T (°C)	G^E_{Ce} (expt. [23])	G^E_{Ce} (calc.)
0.00101	717	−136	−142
0.00084	700	−138	−142
0.00076	680	−140	−143
0.00145	672	−141	−143
0.00082	665	−142	−143
0.00061	642	−144	−143
0.00042	632	−145	−144
0.00014	611	−148	−144
0.00037	600	−149	−144
0.00027	581	−151	−144
0.00021	562	−153	−145
0.00010	530	−157	−145

Table 7
Invariant reactions in the Ce–Zn system

Invariant reaction	Calculated values			
	T (°C)	X_1	X_2	X_3
Liq = Ce(fcc) + CeZn	495.5	0.190	0.000	0.500
Liq = CeZn	825.0	0.500	0.500	
Liq = CeZn + $CeZn_2$	802.7	0.565	0.500	0.667
Liq = $CeZn_2$	874.7	0.667	0.667	
Liq + $CeZn_2$ = $CeZn_3$	812.9	0.729	0.667	0.750
Liq + $CeZn_3$ = Ce_3Zn_{11}	820.3	0.763	0.750	0.786
Liq + $Ce_{13}Zn_{58}$ = Ce_3Zn_{11}	847.6	0.775	0.817	0.786
Liq + $CeZn_5$ = $Ce_{13}Zn_{58}$	870.6	0.796	0.833	0.817
Liq + Ce_3Zn_{22} = $CeZn_5$	886.7	0.810	0.880	0.833
Liq + Ce_2Zn_{17} = Ce_3Zn_{22}	962.1	0.861	0.895	0.880
Liq = Ce_2Zn_{17}	981.7	0.895	0.895	
Liq + Ce_2Zn_{17} = $CeZn_{11}$	795.9	0.994	0.895	0.917
Liq = $CeZn_{11}$ + Zn	419.6	0.999	0.917	1.000

X = mol fraction Zn.

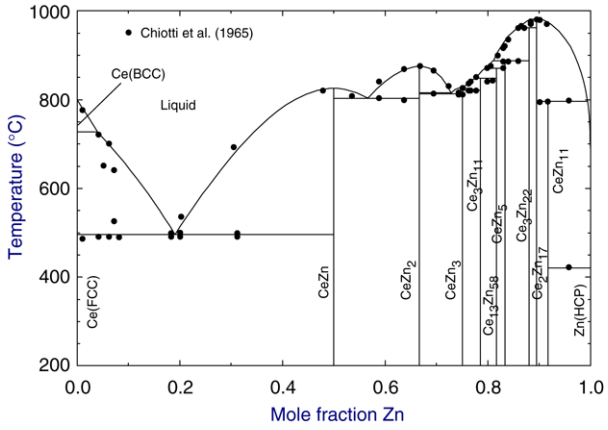

Fig. 16. Ce–Zn phase diagram.

The calculated enthalpy and entropy of mixing curves for the liquid phase of the Ce–Zn system at 1000 °C are shown in Figs. 19 and 20.

Table 6 compares experimental partial excess Gibbs energies of cerium obtained by Lebedev et al. [33,34] for Zn-rich alloys with the corresponding values calculated using the present assessed parameters. As for the Y–Zn system, there is reasonable agreement between experimental and calculated values, particularly for temperatures in the middle of the experimental temperature range. For this system too, however, the experimental data from Lebedev et al. [33,34] correspond to an unreasonably large limiting partial excess entropy of cerium of approximately −112 J/mol K. The value of about −16 J/mol K obtained from the present assessment is more reasonable.

Table A.1
Crystallographic information [27] for the binary phases in the Ca–Zn, Sr–Zn, Y–Zn and Ce–Zn systems

Phase	Strukturbericht	Prototype	Pearson symbol	Space group	Model[a]	Note
Liquid	–	–	–	–	MQM	
FCC	A1	Cu	*cF*4	$Fm\bar{3}m$	Random mixing	Ca, Sr, Ce have stable FCC phase
BCC	A2	W	*cI*2	$Im\bar{3}m$	Random mixing	Ca, Sr, Y, Ce have stable BCC phase
HCP	A3	Mg	*hP*2	$P6_3/mmc$	Random mixing	Y has stable HCP phase
Ca_3Zn	$E1_a$	BRe_3	*oC*16	*Cmcm*	ST	
Ca_5Zn_3	$D8_1$	Cr_5B_3	*tI*32	*I*4/*mcm*	ST	
CaZn	B_f	CrB	*oC*8	*Cmcm*	ST	
$CaZn_2$		$CeCu_2$	*oI*12	*Imma*	ST	
$CaZn_3$		$CaZn_3$	*hP*32	$P6_3/mmc$	ST	
$CaZn_5$	$D2_d$	$CaCu_5$	*hP*6	*P*6/*mmm*	ST	
$CaZn_{11}$		$BaCd_{11}$	*tI*48	$I4_1/amd$	ST	
$CaZn_{13}$	$D2_3$	$NaZn_{13}$	*cF*112	*Fm*3*c*	ST	
SrZn	B27	FeB	*oP*8	*Pnma*	ST	
$SrZn_2$		$CeCu_2$	*oI*12	*Imma*	ST	
$SrZn_5$	$D2_d$	$CaCu_5$	*hP*6	*P*6/*mmm*	ST	
$SrZn_{13}$	$D2_3$	$NaZn_{13}$	*cF*112	*Fm*3*c*	ST	
YZn	B2	CsCl	*cP*2	*Pm*3*m*	ST	
YZn_2			*oI*12	*Imma*	ST	
YZn_3			*oP*16	*Pnma*	ST	
Y_3Zn_{11}			*oI*28	*Immm*	ST	
Y_2Zn_9					ST	
YZn_5			*hP*36	$P6_3/mmc$	ST	
Y_2Zn_{17}			*hP*38	$P6_3/mmc$	ST	
YZn_{12}	$D2_b$	$Mn_{12}Th$	*tI*26	*I*4/*mmm*	ST	
CeZn	B2	CsCl	*cP*2	*Pm*3*m*	ST	
$CeZn_2$			*oI*12	*Imma*	ST	
$CeZn_3$			*oC*16	*Cmcm*	ST	
Ce_3Zn_{11}			*oI*28	*Immm*	ST	
$Ce_{13}Zn_{58}$			*hP*142	$P6_3mc$	ST	
$CeZn_5$	$D2_d$	$CaCu_5$	*hP*6	*P*6/*mmm*	ST	
Ce_3Zn_{22}			*tI*100	$I4_1/amd$	ST	
Ce_2Zn_{17}			*hR*19	*R*3*m*	ST	
$CeZn_{11}$			*tI*48	$I4_1/amd$	ST	

[a] MQM = Modified Quasichemical Model [1], ST = Stoichiometric compound.

Table A.2
Optimized model parameters of all phases in the Ca–Zn, Sr–Zn, Y–Zn and Ce–Zn systems (J/mol) (Data for the pure elements Ca, Sr, Y, Ce, Zn, in stable and non-stable structures, were taken from Ref. [35])

Liquid alloy				
Coordination numbers				Gibbs energies of pair exchange reactions
i	j	Z_{ij}^{i}	Z_{ij}^{j}	
Ca	Zn	3	6	$\Delta g_{CaZn} = -20920 + 5.8576T - 8995.6X_{CaCa} - 10669.2X_{ZnZn}$
Sr	Zn	3	6	$\Delta g_{SrZn} = -20920 + 5.6484T - 1882.8X_{SrSr} - 8786.4X_{ZnZn} + 1966.48X_{SrSr}^{2} - 2092X_{ZnZn}^{2}$
Y	Zn	4	6	$\Delta g_{YZn} = -28451.2 + 5.8576T - 8242.48X_{YY} - 15480.8X_{ZnZn}$
Ce	Zn	3	6	$\Delta g_{CeZn} = -36400.8 + 5.8576T - 9204.8X_{CeCe} - 16736X_{ZnZn}$
Stoichiometric compounds				
Compound		$H^{\circ}_{298.15\,K}$ (J/mol)	$S^{\circ}_{298.15\,K}$ (J/mol K)	C_p(J/mol K)
Ca_3Zn		−36353	163.85	$C_p = 3 \times C_p(Ca,FCC\text{-}A1) + C_p(Zn,HCP\text{-}Zn)$
Ca_5Zn_3		−108144	326.10	$C_p = 5 \times C_p(Ca,FCC\text{-}A1) + 3 \times C_p(Zn,HCP\text{-}Zn)$
CaZn		−35605	79.10	$C_p = C_p(Ca,FCC\text{-}A1) + C_p(Zn,HCP\text{-}Zn)$
$CaZn_2$		−65952	118.20	$C_p = C_p(Ca,FCC\text{-}A1) + 2 \times C_p(Zn,HCP\text{-}Zn)$
$CaZn_3$		−83210	154.86	$C_p = C_p(Ca,FCC\text{-}A1) + 3 \times C_p(Zn,HCP\text{-}Zn)$
$CaZn_5$		−118083	226.35	$C_p = C_p(Ca,FCC\text{-}A1) + 5 \times C_p(Zn,HCP\text{-}Zn)$
$CaZn_{11}$		−210647	421.70	$C_p = C_p(Ca,FCC\text{-}A1) + 11 \times C_p(Zn,HCP\text{-}Zn)$
$CaZn_{13}$		−209934	511.72	$C_p = C_p(Ca,FCC\text{-}A1) + 13 \times C_p(Zn,HCP\text{-}Zn)$
SrZn		−36700	87.30	$C_p = C_p(Sr,FCC\text{-}A1) + C_p(Zn,HCP\text{-}Zn)$
$SrZn_2$		−69700	120.46	$C_p = C_p(Sr,FCC\text{-}A1) + 2 \times C_p(Zn,HCP\text{-}Zn)$
$SrZn_5$		−146500	206.70	$C_p = C_p(Sr,FCC\text{-}A1) + 5 \times C_p(Zn,HCP\text{-}Zn)$
$SrZn_{13}$		−250074	514.00	$C_p = C_p(Sr,FCC\text{-}A1) + 13 \times C_p(Zn,HCP\text{-}Zn)$
YZn		−88010	63.80	$C_p = C_p(Y,HCP\text{-}A3) + C_p(Zn,HCP\text{-}Zn)$
YZn_2(lt)		−155368	77.64	$C_p = C_p(Y,HCP\text{-}A3) + 2 \times C_p(Zn,HCP\text{-}Zn)$
YZn_2(ht)		−147000	85.82	$C_p = C_p(Y,HCP\text{-}A3) + 2 \times C_p(Zn,HCP\text{-}Zn)$
YZn_3		−178000	112.16	$C_p = C_p(Y,HCP\text{-}A3) + 3 \times C_p(Zn,HCP\text{-}Zn)$
Y_3Zn_{11}		−580550	400.75	$C_p = 3 \times C_p(Y,HCP\text{-}A3) + 11 \times C_p(Zn,HCP\text{-}Zn)$
Y_2Zn_9		−426600	317.99	$C_p = 2 \times C_p(Y,HCP\text{-}A3) + 9 \times C_p(Zn,HCP\text{-}Zn)$
YZn_5		−225420	173.31	$C_p = C_p(Y,HCP\text{-}A3) + 5 \times C_p(Zn,HCP\text{-}Zn)$
Y_2Zn_{17}		−515000	640.00	$C_p = 2 \times C_p(Y,HCP\text{-}A3) + 17 \times C_p(Zn,HCP\text{-}Zn)$
YZn_{12}		−268160	465.00	$C_p = C_p(Y,HCP\text{-}A3) + 12 \times C_p(Zn,HCP\text{-}Zn)$
CeZn		−73050	101.21	$C_p = C_p(Ce,FCC\text{-}A1) + C_p(Zn,HCP\text{-}Zn)$
$CeZn_2$		−119850	137.44	$C_p = C_p(Ce,FCC\text{-}A1) + 2 \times C_p(Zn,HCP\text{-}Zn)$
$CeZn_3$		−155950	169.03	$C_p = C_p(Ce,FCC\text{-}A1) + 3 \times C_p(Zn,HCP\text{-}Zn)$
Ce_3Zn_{11}		−526583	578.23	$C_p = 3 \times C_p(Ce,FCC\text{-}A1) + 11 \times C_p(Zn,HCP\text{-}Zn)$
$Ce_{13}Zn_{58}$		−2608888	2817.92	$C_p = 13 \times C_p(Ce,FCC\text{-}A1) + 58 \times C_p(Zn,HCP\text{-}Zn)$
$CeZn_5$		−213700	235.56	$C_p = C_p(Ce,FCC\text{-}A1) + 5 \times C_p(Zn,HCP\text{-}Zn)$
Ce_3Zn_{22}		−779194	969.01	$C_p = 3 \times C_p(Ce,FCC\text{-}A1) + 22 \times C_p(Zn,HCP\text{-}Zn)$
Ce_2Zn_{17}		−567380	725.51	$C_p = 2 \times C_p(Ce,FCC\text{-}A1) + 17 \times C_p(Zn,HCP\text{-}Zn)$
$CeZn_{11}$		−307890	453.75	$C_p = C_p(Ce,\,FCC-A1) + 11 \times C_p(Zn,HCP\text{-}Zn)$

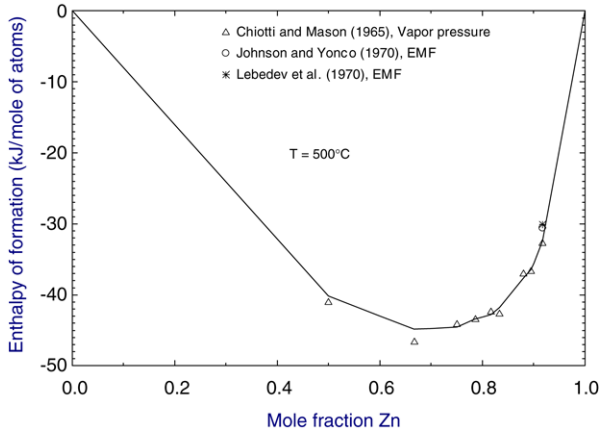

Fig. 17. Enthalpies of formation at 500 °C for the compounds in the Ce–Zn system. Reference states are Ce(fcc) and Zn(liquid).

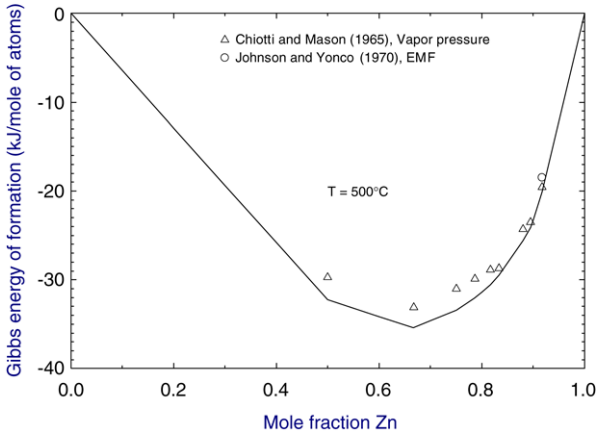

Fig. 18. Gibbs energies of formation at 500 °C for the compounds in the Ce–Zn system. Reference states are Ce(fcc) and Zn(liquid).

Table 7 presents the calculated compositions and temperatures for the invariant reactions in the Ce–Zn system using the present assessed parameters.

Acknowledgements

Financial support in the form of a CRD grant from the Natural Sciences and Engineering Research Council of Canada (NSERC) and from General Motors of Canada is gratefully acknowledged.

Appendix

See Tables A.1 and A.2.

References

[1] Y.-B. Kang, A.D. Pelton, P. Chartrand, P. Spencer, C.D. Fuerst, J. Phase Equilibria Diffusion 28 (2007) 342;

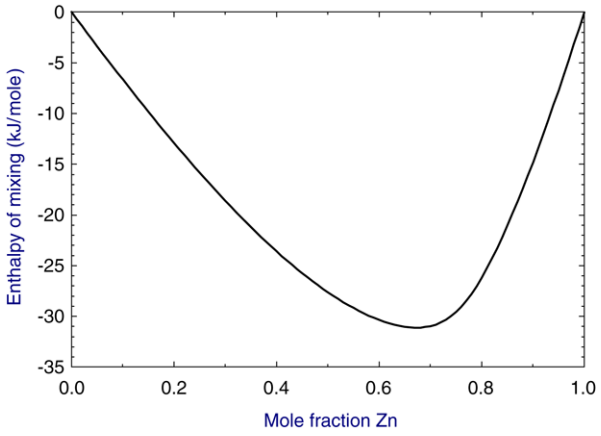

Fig. 19. Enthalpy of mixing of liquid Ce–Zn alloys at 1000 °C.

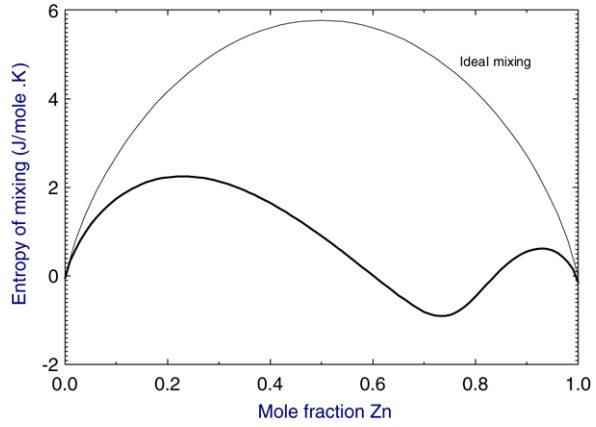

Fig. 20. Entropy of mixing of liquid Ce–Zn alloys at 1000 °C.

Y.-B. Kang, A.D. Pelton, P. Chartrand, P. Spencer, C.D. Fuerst, Metall. Mater. Trans. A 38A (2007) 1231.

[2] A.D. Pelton, S.A. Degterov, G. Eriksson, C. Robelin, Y. Dessureault, Metall. Mater. Trans. B. 31B (2000) 651.
[3] A.D. Pelton, Y.-B. Kang, Int. J. Mater. Res. (formerly Z. Metallkd.) 98 (2007) 907.
[4] V.P. Itkin, C.B. Alcock, Bull. Alloy Phase Diagrams 11 (1990) 328.
[5] A.F. Messing, M.D. Adams, R.K. Steunenberg, Trans. ASM 56 (1963) 345.
[6] C.O. Brubaker, Z.-K. Liu, CALPHAD 26 (2001) 381.
[7] J. Delcet, J.J. Egan, Metall. Trans. 9B (1978) 729.
[8] P. Chiotti, R.J. Hecht, Trans. AIME 239 (1967) 536.
[9] P. Chiotti, G.J. Gartner, E.R. Stevens, Y. Saito, J. Chem. Eng. Data 11 (1966) 571.
[10] G. Bruzzone, F. Merlo, J. Less-Common Met. 92 (1983) 75.
[11] F. Shunk, Structures of Binary Alloys, Metallurgiya, Moscow, 1973.
[12] A.V. Volkovich, A.V. Krivopushkin, I.F. Nichkov, Sov. Non-Ferrous Met. Res. 6 (1978) 245.
[13] Y. Zhong, K. Ozturk, Z-K. Liu, J. Phase Equilibria 24 (2003) 340.
[14] P. Chiotti, J.T. Mason, K.J. Gill, Trans. TMS-AIME 227 (1963) 910.
[15] K.S. Harsha, Ph.D. Thesis, Pennsylvania State University, University Park, PA, 1964.
[16] E. Veleckis, R.V. Schablaske, I. Johnson, H.M. Feder, Trans. TMS-AIME 239 (1967) 58.
[17] G. Bruzzone, M.L. Fornasini, F. Merlo, J. Less-Common Met. 22 (1970) 253.
[18] M.L. Fornasini, J. Less-Common Met. 25 (1971) 329.
[19] E. Ryba, Transformation in AB_2 Intermetallic Compounds, US Atomic Energy Comm. Report COO-3415-3, 1963.
[20] J.T. Mason, P. Chiotti, Metall. Trans. 7A (1976) 287.
[21] V.P. Butorov, I.F. Nichkov, E.A. Novikov, S.P. Raspopin, Izv. Vyssh. Ucheb. Zaved., Tsvetn. Met. 15 (1973) 96.
[22] Y. Hoshino, J.A. Plambeck, Canadian J. Chem. 48 (1970) 685.
[23] L.F. Yamschikov, V.A. Lebedev, N.F. Nichkov, Izv. Akad. Nauk SSSR, Metally 1 (1979) 83.
[24] C. Marquina, N.H. Kim-Ngan, K. Bakker, R.J. Radwanski, T.H. Jacobs, K.H.J. Buschow, J.J.M. Franse, M.R. Ibarra, J. Phys. Condens. Matter 5 (1993) 2009.
[25] M. Morishita, H. Yamamoto, K. Tsuboki, T. Horike, Int. J. Mater. Res. (formerly Z. Metallkd.) 98 (2007) 10.
[26] G. Shao, V. Varsani, Z. Fan, CALPHAD 30 (2006) 286.
[27] H. Okamoto (Ed.), Binary Alloy Phase Diagrams, second edition plus updates, ASM, 1996.
[28] P. Chiotti, J.T. Mason, K.J. Gill, Trans. TMS-AIME 233 (1965) 786.
[29] G. Bruzzone, M.L. Fornasini, F. Merlo, J. Less-Common Met. 22 (1970) 253.
[30] E. Veleckis, C.L. Rosen, H.M. Feder, J. Phys. Chem. 65 (1961) 2127.
[31] P.I. Kripyakevich, Yu.B. Kuz'ma, N.S. Ugrin, Zh. Struk. Khim. 8 (1967) 703; TR: J. Struct. Chem. 8 (1967) 632 (in Russian).
[32] I. Johnson, R.M. Yonco, Met. Trans. 1 (1970) 905.
[33] V.A. Lebedev, I.F. Nichkov, S.P. Raspopin, B.G. Semenov, Russ. Metall. 5 (1970) 65.
[34] V.A. Lebedev, I.F. Nichkov, S.P. Raspopin, R.Kh. Mullayanov, B.G. Semenov, Russ. J. Phys. Chem. 45 (1971) 1126.
[35] A.T. Dinsdale, SGTE Data for Pure Elements, CALPHAD 15 (4) (1991) 317–425. Plus updates (private communication), 2000. http://www.sgte.org.